LASER BENDING OF MICRO TUBES

Kumar Chandan, Saha P and Mishra P K

Laser Processing Laboratory, Department of Mechanical Engineering
Indian Institute of Technology, Kharagpur 721 302, India

Email : psaha@mech.iitkgp.ernet.in, pkmishra@mech.iitkgp.ernet.in

Abstract
Laser bending is a non-contact flexible forming technique. It is preferred to conventional bending techniques due to the high level of accuracy, repeatability and high degree of control offered by the process. In laser tube bending process the stresses are generated due to heating, which eventually leads to plastic deformation. The compressive plastic strain developed during the process causes the bending of the tubes in the direction of the laser beam. Micro tube bending is rapidly finding applications in MEMS, medical and other technological fields. However, the process has yet not been studied in detail. In order to have better understanding of the parameters that govern the process of laser bending of Micro tubes, experiments have been conducted to bend them using a pulsed Nd-YAG laser. The experimentations necessitated design and fabrication of a set up to facilitate the bending. The parameters involved in the bending of micro tubes have been studied in detail. The experimental results have been compared with the results obtained by simulation of the experiments, under the same conditions, by both analytical and numerical approach.

Keywords: Laser bending, Bending angle, Micro tube, Pulsed Laser, Pulse-energy

1. INTRODUCTION

Laser forming has become a viable process for the shaping of metallic components, as a means of rapid prototyping and of adjusting and aligning. The laser forming process is of significant value to industries that previously relied on expensive stamping dies and presses for prototype evaluations, relevant industry sectors include aerospace, automotive, and microelectronics. In contrast to conventional forming techniques this method requires no mechanical contact and hence offers many of the advantages of process flexibility associated with other laser manufacturing techniques such as laser cutting and marking. Laser forming can produce metallic, predetermined shapes with minimal distortion. The process is similar to the well established torch flame bending used on large sheet material in the ship building industry but a great deal more control on the final product can be achieved. The Laser forming process is realized by introducing thermal stresses into the surface of a work piece. These internal stresses induce plastic strains bending the material or result in local elastic plastic buckling. Micro tube bending is a process in which laser-induced thermal distortion is used to bend micro tubes without external forces. Laser bending of micro tubes offers more flexibility and is more advantageous as compared to the conventional means of bending.

Laser bending mechanisms are described in [1, 2], the laser bending mechanisms and the laser bending process have been

simulated [3, 4], and the variation of the influencing factors on the laser bending process have been discussed [5, 6]. Kraus [7] conducted a finite element modeling study of laser bending of square cross-section tubes and investigated the heating sequence. It was found that although the process is dominated by the upsetting mechanism, an inhomogeneous plastic zone exists at the beginning of the scanning. Li and Yao [8] explained the mechanism of laser tube bending by stress analysis. Hao and Li [9] developed an analytical model to predict the bending angles for laser tube bending and verified it by experiments. It was concluded that the laser induced bending angle increases linearly with the increase of laser power.
Bending of micro tubes using laser has yet not been reported in literatures. In the present work laser bending of micro tubes has been carried out and studied in detail. Both analytical and numerical approach have been adopted to study the process of bending micro tubes using pulsed Laser.

2. MODELING

Laser bending is regarded as a very complex thermo-physical process due to the fast variation in temperature during laser processing and subsequent elasto–plastic deformation. The essence of it is the interaction of thermo-mechanical coupling and the behavior of the plastic yielding of material under the conditions of intense heat flux, high temperature and a varying high temperature gradient.

2.1 Numerical Modeling

Numerical modeling of the heating phase was done using ANSYS code. Wherein, the first step is to model the temperature distribution resulting from the heating. This modeling was done for Hypodermic needles (Austenitic Stainless Steel - SS304). In the thermal analysis, equilibrium of heat flow in the interior of the work piece is given by

$$\rho c \dot{T} = \nabla(k \nabla T) + q_{ab}$$

Where, ρ is the density is the thermal conductivity, T is the temperature and q_{ab} is the rate of heat generated per unit volume.

The Boundary conditions applied are

Convection

$$Q_{co} = h_c (T - T_\infty) \mid_{r=R_o}$$

$$Q_{ci} = h_c (T - T_\infty) \mid_{r=R_i}$$

Radiation

$$Q_{ro} = 5.67 x 10^{-8} \varepsilon (T^4 - T_\infty^4) \mid_{r=R_o}$$

$$Q_{ri} = 5.67 x 10^{-8} \varepsilon (T^4 - T_\infty^4) \mid_{r=R_i}$$

Heat Flux

$$-K \frac{\partial T}{\partial r} \mid_{r=R_o} = \eta P \quad 0 < \theta \leq \theta_0 \;\&\; 0 < Z \leq Z_0$$

Where Q_c is the heat loss through convection, Q_r is the heat loss due to radiation, h_c is the coefficient of convective heat transfer, ε is the emissivity, P is the laser power, η is the absorptivity, R_0 is the Outer Radius of the micro tube and R_i is the inner radius of the micro tube and.

Initial Condition

$T\ (t=0) = 25^{o}C$

Due to the temperature increase during laser irradiation material properties change considerably. The temperature dependent values of the material properties, used for the simulation, were taken from reference [10]. The heated region can be considered to be as a set of cubical elements. Due to non-uniform temperature rise in the heated region each of the cubical elements expand by different amounts. In order to fit together to form a continuous body, distortions in the elements and consequently stresses occur in the heated region. These stresses may exceed the Yield Strength at some point of

time due to considerable fall in the value of the Yield Strength at high temperatures. This leads to plastic deformation. Hence there is a need to evaluate the stresses (σ) and the strains (ε) occurring due to the non-uniform rise in temperature. Stresses and strains are calculated using the following relations [11].

Equilibrium Equation

$$\sigma_{ji,j} + F_i = 0 \qquad (i, j = x, y, z)$$

Strain-Displacement Equation

$$\varepsilon_{ij} = \frac{1}{2}(u_{i,j} + u_{j,i}) \qquad (i, j = x, y, z)$$

Governing Equation of thermo-elasticity

$$\sigma_{i,j=2\mu\varepsilon_{ij}+(\lambda e-\beta\tau)\delta_{ij}} \qquad (i, j = x, y, z)$$

where μ is Poison's ratio.

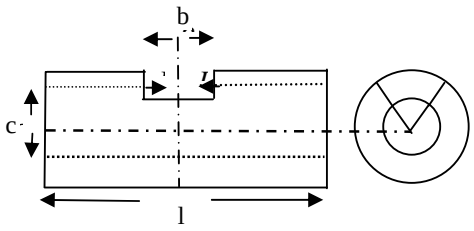

Fig. 1: Simplified Theoretical Model (*Hao And Li, 2003*)

2.2 Theoretical Modeling

The theoretical model proposed by *Hao and Li, 2003* [9] has been used for the purpose of calculating the bending angle (Figure 1). Wherein, bending angle is given by the strain difference between the heated and the unheated part.

The average temperature ΔT of the heated region is found by numerical simulation of the thermal process. The Strain in the heated part after cooling is given by

$$\varepsilon_h = -\alpha\Delta T/2 + F/S_1E$$

Where S_1 is the cross-sectional area of the heated part and ΔT the temperature rise of the heated part. The strain in the unheated part after cooling is given by

$$\varepsilon_{uh} = -F/S_2E$$

Where S_2 is the cross-sectional area of the unheated part.

$$F = Z\sigma y/C$$

Where Z is the plastic modulus of the unheated part.

$$\theta = b\,(\varepsilon_{uh} - \varepsilon_h)/\,C$$

The thickness of the tube in the heated region increases to $t_{new} = t\,(1- \varepsilon_h)$.The total bending angle is the summation of all angles obtained in each pulse.

3. EXPERIMENTS

Experiments were performed using pulsed-Nd-Yag laser on hypodermic needles with outer diameter equal to 1.032 mm and thickness equal to 0.143 mm. The simple set-up designed for the purpose consists of a bracket, collet and a stepper motor (Figure 2). In the present work stepper motor was not made use of. However, future work going on this field requires the stepper motor to provide angular velocity to the micro tube while laser beam would be made incident on the surface by $C0_2$ Laser.

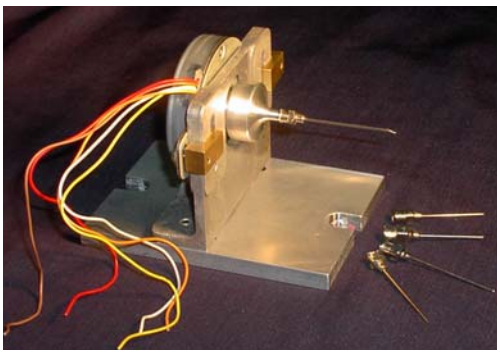

Fig. 2: Experimental Set-Up

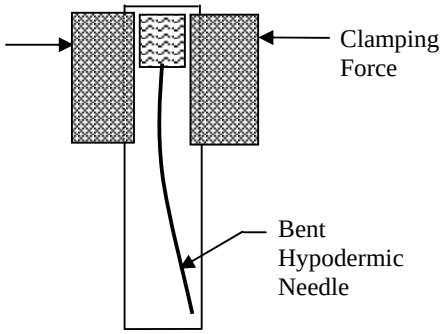

Fig. 3: Top View of the set-up for measuring bending angle

Bending was measured with the help of microscope having an attached display monitor. Figure 3 shows the Top View of the simple set-up for measuring the maximum bending angle. By observing through a microscope and moving along the length in very small steps, maximum bending angle was measured.

Table 1 shows the experiments that were conducted by varying the Pulse-Energy and Pulse On-time while the laser beam diameter was kept constant at 700μm

4. RESULTS AND DISCUSSION

4.1 Simulation

The area irradiated with laser tends to expand quickly, while other areas still in lower temperature tend to expand in a small scale. The difference of expansion and the integrality of the material cause a thermal stress in the material. The heated area exerts pressure to its surrounding area and the surrounding area exerts pressure on the heated area inversely. That is, the material in heated area is in thermal expansion and mechanical elastic compression.

Table 1: Experiments Conducted Using Pulsed Laser

Serial number	Pulse energy (J)	Pulse width (ms)	Bending angle (degree)	Remarks
1	5.33	10	3.06	Total 10 pulses at a distance of 50 mm from the root of the needle
2	5.33	10	5.15	10 pulses at 6 positions. Each position at an offset of 1 mm
3	5.48	10	3.6	10 pulses at 5 positions. Each position at an offset of 1 mm
4	4.6	10	2.4	10 pulses at 5 positions. Each position at an offset of 1 mm
5	3.82	10	1.7	10 pulses at 5 positions. Each position at an offset of 1 mm
6	4.6	12	1.6	10 pulses at 5 positions. Each position at an offset of 1 mm
7	4.68	8	2.96	10 pulses at 5 positions. Each position at an offset of 1 mm

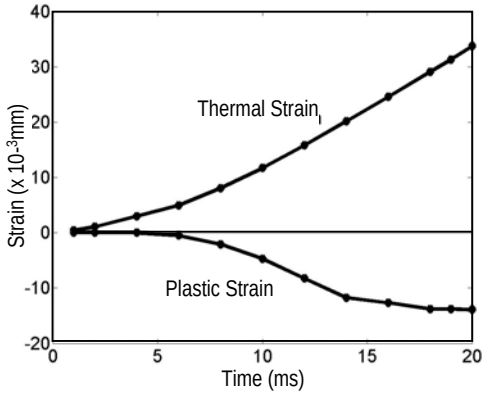

Fig. 4: The Numerical Simulation of the Heating Phase Showing Increase in Tensile Thermal Strain and Compressive Plastic Strain with the Increase in Heating Time

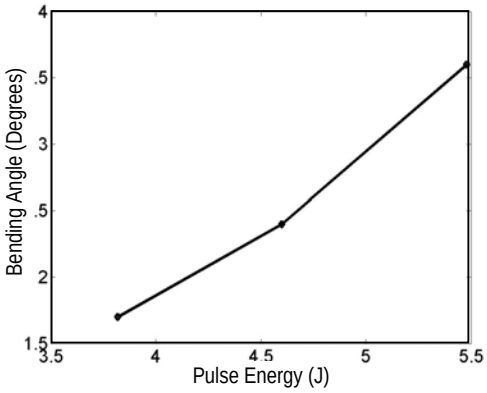

Fig. 5: Influence of Pulse-Energy on Bending Angle

Figure 4 shows the plot of thermal strain & plastic strain versus heating time. It was observed that initially the thermal strain increases while the plastic strain is zero. At a certain temperature, which is dependent upon the material and the geometry, the thermal strains reach the maximum elastic strain that the material can endure. Further increase in the temperature would result in a conversion of the thermal expansion into plastic compressive strains. When the heating continues, the thermal expansion begins to convert into plastic compression until the cooling period begins.

As seen in figure 4 thermal strain constantly rises during heating and so does the plastic strain. In the time steps 1, 2, 4 ms the plastic strain is zero since till that time yielding has not taken place. After t = 4ms yielding takes place and plastic strain rises. In the initial stages of heating due to tensile thermal strain the heated material tends to expand but is restricted by the neighboring material. Hence in the initial stages 'no' or only a small amount of bending may be observed in a direction away from the laser. As time increases the tensile thermal strain increases and so does the compressive plastic strain. The elastic strain was negligible as compared to the plastic strain. However after cooling the thermal strain reduces to zero. Also, compressive plastic strain recovers a little during cooling.

It is during cooling that the tube bends due to the shrinkage force resulting from cooling and the axial compressive plastic strain developed during the heating phase.

4.2 Experimental Investigation

The experimental values clearly reveal that with the increase in energy per pulse the bending angle increases. Figure 5 shows the increase in value of bending angle with the increase in Energy per pulse keeping the beam diameter and Pulse On-time constant. This can be explained by the fact that with the increase in energy per pulse the bulk temperature rise of the heated zone also increases leading to increase in thermal and plastic strain during heating. A comparison between the bending angles obtained in experiment no.4 (Pulse-Energy = 4.6 J, Pulse-On time = 10ms, Bending angle = 2.4^0) and experiment no.6 (Pulse-Energy = 4.6 J, Pulse-On time = 12ms, Bending angle = 1.6^0) reveals that with the decrease in Pulse On-time keeping the

energy per pulse constant bending angle increases. This can be explained by the fact that with the decrease in Pulse On-time, the peak temperature obtained during the heating time would be larger and hence would lead to more bending.

4.3 Comparison between Theoretical Value and Experimental Value

Using the parameters of Experiment No. 1 as input the theoretical model was used to calculate the maximum bending angle. Table 2 shows the calculated bending angle for each pulse.

Table 2: Calculated Bending Angles for Each Pulse

Pulse number	Bending angle (degree)
1st	0.773
2nd	0.762
3rd	0.751
4th	0.741
5th	0.730
6th	0.721
7th	0.710
8th	0.700
9th	0.691
10th	0.682

Total bending angle (calculated)

$$= \sum_{i=1}^{i=10} \theta_i = 7.26^0$$

Experimentally measured bending angle

$$= 3.06^0$$

The theoretically calculated bending angle was found to be larger than the experimentally measured bending angle. The main cause responsible for differences between the calculated and the experimental value can be explained by the fact that melting had taken place while performing the experiments. Melting of the surface in the heated region leads to a change of state from solid to liquid and in some cases liquid to vapor. The change of state from liquid to vapor may lead to a large change in volume and the vapor exerts a recoil pressure in order to escape away. The axial component of the recoil force opposes the compressive axial plastic strain developed during heating. Moreover, the moment melting takes place the surface integrity is lost. Thus finding no resistance, the thermal stresses cause an initial bending of the tube in the opposite direction, which is sometimes referred to as counter bending.

5. CONCLUSION

The development of stress and strain during laser micro tube bending had been investigated both experimentally and analytically. The mechanism of micro tube bending has been discussed based on simulation and experimental results. The following conclusions can be drawn from the present work.

For the same amount of angularly heated region, the thinner the tube lesser will be the bending moment experienced by the unheated part. Thus even a small amount of melting would hamper the bending process severely.

The laser local heating causes large thermal expansion and low yield stress on the upper surface under the high temperature. Subsequently the heated region of the material produces compressive plastic deformation.

During the Pulse Off-time the temperature on the upper surface drops very quickly and material contracts. The material of the heated region of the tube become shorter than that of the unheated region after cooling and thus the difference in length enables the tube to bend.

The main factors affecting the bending process using a pulsed laser are Pulse-

Energy, duration of heating or Pulse-On time, and Spot size of the incident laser beam.

Increase in Pulse-Energy keeping the heating duration constant causes the bending angle to increase.

Decrease in Pulse On-time keeping the Pulse-energy constant causes the bending angle to increase.

6. REFERENCES

1. **Vollertsen F.** (1994), "Mechanisms and Models for Laser Forming", in: *Proceedings of the LANE'94*, M. Geiger, F. Vollertsen (Eds.), Meisenback Bamberg, 345–359.

2. **Vollertsen F. and Rodle M.** (1994), "Model for the Temperature Gradient Mechanism of Laser Bending", in: *Proceedings of the LANE'94*, M. Geiger, F. Vollertsen (Eds.), Meisenback Bamberg, 371–378.

3. **Vollertsen F., Geiger M. and Li W.M.** (1993), "FDM and FEM Simulation of Laser Forming - A Comparative Study", in: *Advanced Technology of Plasticity*, Z.R. Wang (Ed.), Vol. 3, 1793–1798.

4. **Alberti N., Fratini L. and Micari F.** (1994), "Numerical Simulation of the Laser Bending Process by a Coupled Thermal Mechanical Analysis", in: *Proceedings of the LANE'94*, M. Geiger, F. Vollertsen (Eds.),, Meisenback Bamberg, 327–336.

5. **Namba Y.** (1986), "Laser Forming in Space", in: *Proceedings of the International Conference on Laser'85*, C.P. Wang (Ed.), 403–407.

6. **Geiger M., Vollertsen F. and Deinzer G.** (1993), "Flexible Straightening of Car Body Shell by Laser Forming", *SAE Paper No. 930279*, 354–361.

7. **Kraus J.** (1997), " Basic Process in Laser Bending of Extrusion using the Upsetting Mechanism", *Proceedings of the LANE 2*, 431–438.

8. **Li W. and Yao Y. L.** (2001), "Laser Bending of Tubes: Mechanism, Analysis and Prediction", *ASME Journal of Manufacturing Science Engg.*, Vol. 123, 674–681.

9. **Hao N. and Li L.** (2003), "An Analytical Model for Laser Tube Bending", *Journal of Applied Surface Science*, 432-436.

10. **Tavassoli A. A.** (1995), "Assessment of Austenitic Stainless Steel", *Fusion and Design Engineering*, Vol. 29, 371-390.

11. **Noda N., Hetnarski R. B., and Tanigawa Y.**, (2003), "*Thermal Stresses*", Taylor and Francis, New York.